PLANFORM MORPHOMETRY OF WELL-PRESERVED MARTIAN AND LUNAR IMPACT CRATERS

W. A. Watters, L. Geiger, M. Fendrock, R. Gibson, and C. Hundal. Whitin Observatory, Wellesley College, 106 Central St., Wellesley, MA, USA (wwatters@wellesley.edu).

Introduction: We present an analysis of crater planform morphometry for simple and complex craters on the Moon and Mars, with the aim illuminating the processes that form craters and modify them over time. Previous work has found that simple craters appear to become more circular with increasing diameter, while complex craters become less circular or exhibit asymmetry that is size-independent [e.g., 1,2]. Using the high-resolution imagery and stereo-derived topography that has become available in recent years (High-Resolution Science Imaging Experiment (HiRISE) [3]; High-resolution Stereo Camera (HRSC) [4]; Wide-Angle Lunar Reconnaissance Orbiter Camera (LROC-WAC) [5]) we measure the diameter scaling of planform shape in detail, arriving at useful constraints for models of impact cratering and planetary surface processes.

Crater databases: We present results from three sets of well-preserved impact craters. Set A are 350 martian simple craters whose rims were measured from HiRISE stereo-derived elevation models, as in [6]. These range in diameter from roughly 25 m to 5 km and are well-preserved with respect to nearby craters but exhibit a range of crater preservation states overall. Preservation has been assessed using a combination of qualitative and quantitative attributes; the best-preserved have been identified as in [6].

Set B is made up of 385 martian complex craters whose rims have been traced manually from orthorectified nadir HRSC images. These craters belong to class 4 of the Robbins & Hynek 2012 crater catalog [7], identified as among the best-preserved complex craters on Mars. These range in diameter from 5 km to 40 km. Finally, set C are lunar complex craters identified as Eratosthenian or younger [8]. The planforms in this case were manually traced from a global LROC WAC mosaic [9] and range in size from 20 km to 160 km.

Methods: Planforms of the martian simple craters (set A) were measured from two morphometric features: (i) the topographic rim crest, and (ii) an elevation contour of the upper cavity wall (corresponding to the highest plane that entirely closes the crater cavity). The topographic rim crest was extracted according to the methods described in [6]: assembled in an automatic fashion from local elevation maxima. Each rim was inspected for errors, and prominent slope breaks were in some cases used to bridge gaps. The use of elevation models is deemed essential for this measurement because it is nearly impossible to confidently identify the crests of rounded rims of small fresh martian craters in imagery alone.

For the complex craters in sets B and C, the rims were traced manually from orthorectified images. Well-preserved complex craters have rims that are readily identified and traced along sharp edges (i.e., in imagery with typical resolutions of < 25 m/pix for HRSC nadir and ~ 100 m/pix for LROC WAC).

Morphometric quantities: This work focuses on measures of planform shape and especially the deviation from radial symmetry. Shape was characterized by measuring the distribution of harmonic amplitudes as in [10] via Fourier decomposition. Unlike that earlier work, craters are assigned to a shape category according to the largest harmonic amplitude (for example, Meteor Crater would be assigned to "4" because its quadratic amplitude is by far the strongest).

Many quantities have been used to measure asymmetry, such as the circularity index and major to minor axis ratio [e.g., 11, 12]. In this abstract, we present results for the average radial deviation (δR): the average absolute difference between a single radius measurement and the average radius for the crater as a whole. In computing δR, care was taken to avoid oversampling the rim with respect to image or DEM resolution.

Results: Figure 1 shows δR as a function of crater diameter (D) on a log-log scale for the martian simple craters of set A, and Figures 2 and 3 show these measurements for the martian and lunar complex craters of sets B and C, respectively. A bootstrap method is provisionally used to estimate the error bars, which represent the full range of δR values for 1000 statistical samples (with replacement). As such, the error bars significantly overestimate the true uncertainty because radius measurements are not independent and uncorrelated.

Martian simple craters classified as "moderately modified" in [6] exhibit a trend $\delta R \sim D^m$, for $m = 0.69 \pm 0.02$. Measuring this relationship for the best-preserved craters lowers the exponent to $m \approx 0.6$. The set B complex craters follow a trend defined by $m = 1.27 \pm 0.06$, and the complex lunar craters of set C fall on a trend given by $m = 1.11 \pm 0.06$. That is, the departure from radial symmetry (as a fraction of overall size) may slightly increase with diameter for complex craters, and certainly decreases for simple craters.

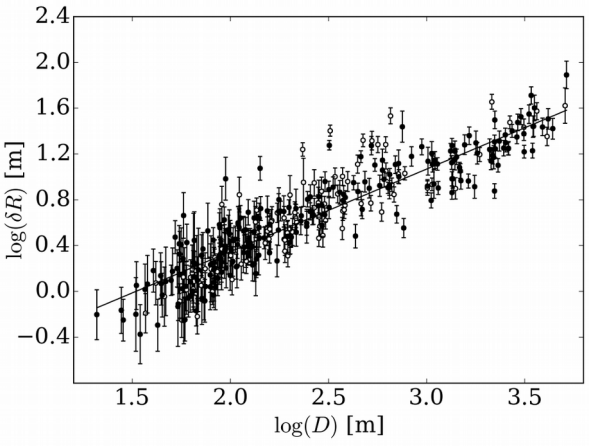

Figure 1. Average radial deviation versus diameter for "moderately modified" ("MM", filled circles) and "heavily modified" simple craters (open circles), as in [6] (N = 350). The fit indicates $\delta R \sim D^m$ for $m \sim 0.69 \pm 0.02$ for MM.

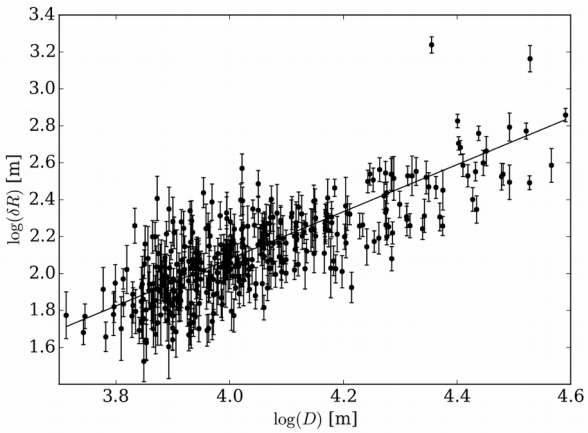

Figure 2. Average radial deviation versus diameter for well-preserved martian complex craters as defined in [7]. (N = 385) The fit indicates $\delta R \sim D^m$ for $m \sim 1.27 \pm 0.06$.

Discussion. The measured planform shape distributions and diameter-dependent trends supply a powerful constraint for models of crater formation and can help to inform our understanding of the role of target strength and strength heterogeneities in crater excavation and collapse. For example, scaling of the form $\delta R \sim D^m$ for $m \sim 1$ might be expected if the average radial size of blocks that fail during crater collapse also scales with crater diameter. A trend closer to $m \sim 0.5$ may result if the excavation flow is sensitive to the integrated influence of strength heterogeneities of uniform size (i.e., akin to the scaling of the sum of uniformly-distributed random numbers).

Martian impact craters not forming in sand targets are influenced by target strength in the excavation stage (for small craters) or collapse stage (for large craters). We have therefore also measured these relationships for craters that occur in relatively strong materials (maria on the Moon and young lava plains on Mars) versus relatively weak materials (crater ejecta, sedimentary basins, and lunar highlands).

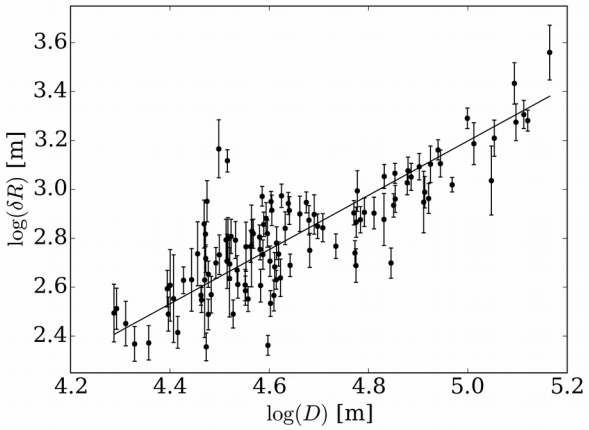

Figure 3. Average radial deviation versus diameter for well-preserved lunar complex craters (N = 112). The fit indicates $\delta R \sim D^m$ for $m \sim 1.11 \pm 0.06$.

References. [1] Ronca, L.B. & Salisbury, J. W. (1966) *Icarus*, *5*, 130-138; [2] Pike R. J. (1977) *Impact & Explosion Cratering*, 489-509; [3] McEwen A. et al., (2007) *JGR-Planets*, *112*, E05S02; [4] Jaumann et al. (2007) *Planet. & Space Sci.*, *55*, 928-952. [5] Robinson, M.S. (2010) *Space Sci. Rev. 150*, 81-124. [6] Watters W. A. et al., (2015) *JGR-Planets*, doi: 10.1002/2014JE004630; [7] Robbins S. & Hynek B. (2012) *JGR-Planets*, *117*, E05004; [8] Kalynn et al. (2013) *GRL*, *40*, *38-42;* [9] Robinson, M. LROC-WAC global mosaic v. 1.1; [10] Eppler, D.T. et al. (1983) *GSA Bulletin*, *94*, 274-291. [11] Calef et al. (2009) *JGR-Planets*, *114*, *E10007;* [12] Murray, J.B. & Guest, J.E. (1970) *Modern Geology, 1, 149-159.*